Correlated motion in the bulk of dense granular flows

Lydie Staron
CNRS-Université Paris VI, Institut Jean Le Rond d'Alembert, 4 place Jussieu, Paris 75252 Cedex 5, France
(Received 14 December 2007; revised manuscript received 14 February 2008; published 15 May 2008)

Numerical simulations of two-dimensional stationary dense granular flows are performed. We check that the system obeys the h_{stop} phenomenology. Focusing on the spatial correlations of the instantaneous velocity fluctuations of the grains, we give evidence of the existence of correlated motion over several grain diameters in the bulk of the flow. Investigating the role of contact friction and restitution, we show that the associated typical length scale λ is essentially independent of the grain properties. Moreover, we show that λ is not controlled by the packing compacity. However, in agreement with previous experimental work, we observe that the correlation length decreases with the shear rate. Computing the flows inertia number I, we show a first-order dependence of λ on I.

DOI: 10.1103/PhysRevE.77.051304 PACS number(s): 45.70.Ht

I. INTRODUCTION

Although ubiquitously present in nature as well as in industrial handling and geotechnics, granular flows still escape physical modeling. An important difficulty in understanding their behavior stems from the dissipation occurring at contacts between the grains, leading to long-lasting interactions and nonlocal energy transfers. These remain a persistent obstacle to the definition of a proper rheology for dense granular flows, which has been up to now a subject of lively debate among scientists [1–8]. The analogy between granular media and gas has led to the application of kinetic theory to derive a granular rheology based on binary collisions between the grains. However, when the flow becomes dense, the granular gas picture does not hold anymore: nonlocal effects appear and control part of the dynamics. A remarkable illustration of these nonlocal effects is the experimental flow law obtained by Pouliquen, which establishes the existence of a minimum thickness h_{stop} necessary for a granular bed to flow on a slope θ [9]. The existence of the length h_{stop} suggests that within this distance, the dissipation induced by the substrate extends to distant grains, implying the existence of spatial correlations. Following this picture, the flow stops when its depth has reached a typical length coinciding with the range of spatial correlations existing in the flow. A model supporting this hypothesis is given in [10], where the flow law observed experimentally is recovered theoretically assuming the existence of correlated motion of the grains under the shape of "granular eddies." Eventually the existence of correlated motion over several grain diameters at the surface of granular flows was demonstrated experimentally in [11]. However, the existence of spatial correlations of a similar scale in the bulk of the flow is not as obvious [12]. While experimental work on stationary granular flows in a rotating drum tends to show that no typical length scale emerges when one considers clusters of correlated grains [14], recent numerical work suggests on the contrary that correlated motion obeys a well-defined spatial organization [13]. However, the associated correlation lengths found in this study do not exceed 1.4 grain diameter and are even found to be smaller than the mean grain diameter. In this present contribution, we investigate the existence of spatial correlations of grain motion over several grain diameters, in agreement with the observation of [11], and try to relate them to the flow characteristics. Therefore, numerical simulations of stationary granular flows using contact dynamics are carried out. The spatial distribution of the grain instantaneous velocity fluctuations is analyzed. While evidence of correlated motion in the bulk of the flows is given, we show that the associated typical length scale λ is essentially independent of the grain properties. Moreover, we show that λ is not controlled by the packing compacity. However, in agreement with [11], we observe that the correlation length decreases with the shear rate. Computing the flow inertia number I, we show a first-order dependence of λ on I.

II. SIMULATIONS

The numerical method applied to simulate the granular flows is the contact dynamics [15]. This algorithm assumes perfectly rigid grains interacting through a Coulomb friction law; the microscopic coefficient of friction μ sets the value of the Coulomb threshold at contact. In addition, a coefficient of restitution, e, sets the amount of energy dissipated in the advent of collision between two grains. The motion of the grains simply obeys the equations of the dynamics while obeying the constraint imposed by the nonsmooth contact laws. This algorithm has already proved successful in reproducing the behavior of granular systems observed experimentally in highly dynamic situations [16]. Further details on the numerical method can be found in [17].

The simulated systems consist of two-dimensional granular beds exhibiting a periodicity in the flow (or x) direction. Since it was experimentally observed that grains in the dimension transverse to the flow do not show a behavior different than in the other dimensions in terms of correlation of their motion [11], we are confident that our results should not be qualitatively affected by the two-dimensional approximation. Grain diameters are uniformly distributed in $[d_{\min}, d_{\max}]$ such as $d_{\max}/d_{\min}=1.5$. The grain mean diameter is denoted d. The beds are initially obtained by random deposition under gravity, leading to a compacity of $\simeq 0.8$. The bottom is made rough by gluing grains of diameter d having the same properties as the free grains. The length ℓ of the bed is fixed

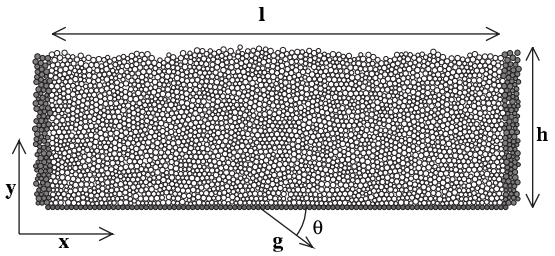

FIG. 1. Example of a simulated granular bed counting 3200 grains of length $\ell=100d$ and depth $h=32d$; grains represented in gray are images of the white ones through periodic boundary conditions in the flow (x) direction.

to $\ell=100d$, and we made sure that this choice has no influence on the dynamics as long as $\ell>15d$. In order to quantify the influence of the depth h of the granular layer on the flow properties, the latter was varied from $h=1d$ to $h=32d$ (corresponding to the deposition of 40 layers of grains). A typical granular bed is shown in Fig. 1. The beds are tilted in the gravity field with the angular velocity $\dot{\theta}=1$ deg s^{-1}, namely, clockwise ($\dot{\theta}=-1$ deg s^{-1}, namely, anticlockwise), so as to induce (stop) the flow of the grains. Stationary flow regimes were obtained at fixed angle θ.

The grain material properties, embodied in the coefficient of restitution, e, and the coefficient of Coulombic friction, μ, were set to $\mu=0.3$ and $e=0.5$ in all the results presented hereafter. However, series of simulations with $\mu=1$ or $\mu=0.05$ and $e=0.5$ or $e=0$ were also carried out to check the influence of these parameters.

III. DEPOSIT FUNCTION

The experimental flow law obtained by Pouliquen establishes the existence of a minimum thickness h_{stop} necessary for a granular bed to flow on a slope θ, where h_{stop} is obtained by measuring the height of the layer of grains remaining once the flow has come to a rest [9]. The resulting function $h_{stop}(\theta)$ is known as the deposit function. Due to the periodicity of our configuration, the height h of the flowing layer is necessarily constant in time (beside the variations due to the compacity). Hence, we rather establish the inverse functions $\theta_{start}(h)$ and $\theta_{stop}(h)$, where θ_{start} (θ_{stop}) is the angle at which an avalanche starts (stops) for a layer of depth h. The procedure was the following. Granular beds of height h varying between $1d$ and $32d$ are slowly tilted clockwise in the gravity field until they reach their angle of avalanche θ_{start} and start flowing. The rotation is maintained until the slope of the beds reaches the arbitrary value $\theta_{start}+3°$ to ensure that the flow is fully developed irrespective of h. An inverse rotation is then applied to decrease the slope θ to the critical value θ_{stop} for which the flow stops. Four independent runs were performed for each value of h to obtain a representative mean value.

The functions $\theta_{stop}(h)$ and $\theta_{start}(h)$ are plotted in Fig. 2 (with θ as the abscissa to conform to the usual representation of the deposit function). All independent runs are represented by open symbols; the average evolution is represented by the solid symbols. In spite of dispersion we recover the behavior classically observed experimentally for chute flows, with a shift of several degrees between θ_{start} and θ_{stop}. In both cases, and in agreement with experimental findings, the points are nicely fitted by the analytical expression

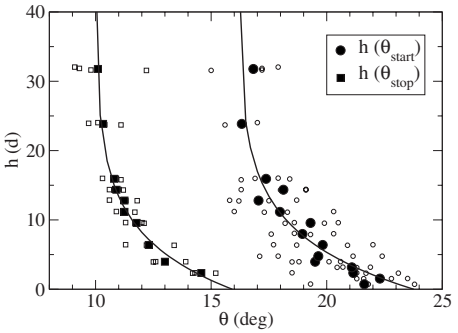

FIG. 2. The deposit function plotted from the measure of θ_{stop} (squares) and θ_{start} (circles) for granular beds of height h varying between $1d$ and $32d$. The straight lines represent the analytical fit. Open symbols represents the data for each independent run, while solid circles are averages for given values of h.

$$\tan\theta=\tan\theta_1+(\tan\theta_2-\tan\theta_1)\exp\left(\frac{h}{L}\right), \qquad (1)$$

where θ_1 (θ_2) is the angle for which h diverges (vanishes). In the case of θ_{stop}, we find $\theta_1=10°$ and $\theta_2=15.9°$, while in the case of θ_{start}, we find $\theta_1=16.2°$ and $\theta_2=23.7°$. These values depend on the properties of the grains μ and e; in the case of θ_{stop}, the choice of the angle $\theta_{start}+3°$ to initiate the anticlockwise rotation is also expected to play a role, which, however, seems not to affect the qualitative behavior of θ_{stop} with h. For both, $L=7.5d$. This value is larger than those obtained experimentally for glass beads [9]; in spite of this slight difference, we do recover the classical h_{stop} phenomenology.

IV. STATIONARY FLOWS

To try to relate the h_{stop} function to the existence of correlated motion of the grains, we carried out series of simulations of steady flows for a granular bed of fixed dimensions $\ell=100d$ and $h=32d$. Therefore, the granular beds are no longer subjected to a rotation in the gravity field, but their slope is kept constant while a stationary flow regime develops. Once the stationary regime is reached (which we assume is the case when the mean grain velocity becomes constant), the flow is recorded and analyzed. All runs of stationary flows are independent one from another.

For grains with properties $\mu=0.3$ and $e=0.5$ (which is the case discussed in the following up to Sec. IV), the stationary regime was observed in the range of slope $\theta=[16.5°,26.5°]$. For slopes larger than 26.5°, the flow is continuously accelerated. For slopes lower than 16.5, the flow rapidly stops. In the following, we focus on the stationary regime. Irrespective of the slope θ, the state of the flowing layer was recorded with a frequency of 10^{-3} (namely, a picture every millisecond) over a period of $70\sqrt{d/g}$. Addi-

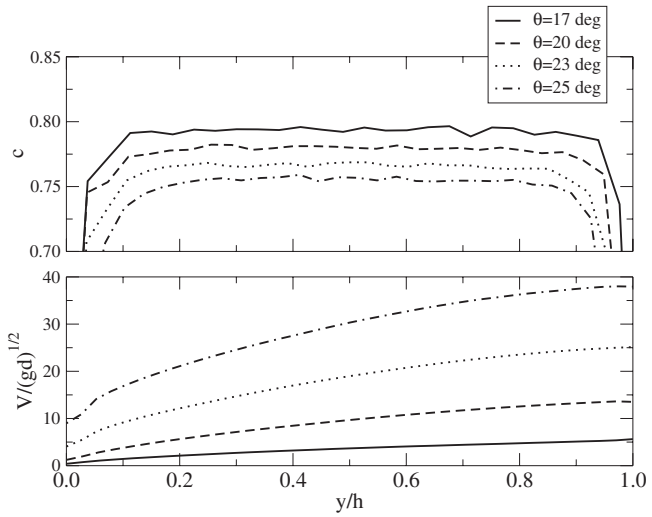

FIG. 3. Time-averaged normalized velocity (bottom graph) and compacity (top graph) profiles in stationary flows for different values of the slope $\theta=17°$, 20°, 23°, and 25°.

tional samplings with different frequency (2×10^{-3}, 10^{-2}, and 2×10^{-2} instead of 10^{-3}) were also recorded to make sure that the results were not affected.

As an illustration, the time-averaged velocity profiles for different slope angles are displayed in Fig. 3 and show a shape compatible with a Bagnold law, in agreement with previous works [1]. The corresponding compacity profiles are shown in the same figure. While the compacity in the mean decreases with the slope, the profiles show no significant variation with depths, besides at the surface and the bottom—namely, the boundaries of the flow.

For the complete series of simulations of stationary flows with $\mu=0.3$ and $e=0.5$, we compute for each run the time-averaged inertia number I [1]:

$$I=\frac{\dot{\gamma}d}{\sqrt{P/\rho}},$$

where $\dot{\gamma}$ is the shear rate, P is the pressure, and ρ is the density. The variation of the inertia number I with the slope

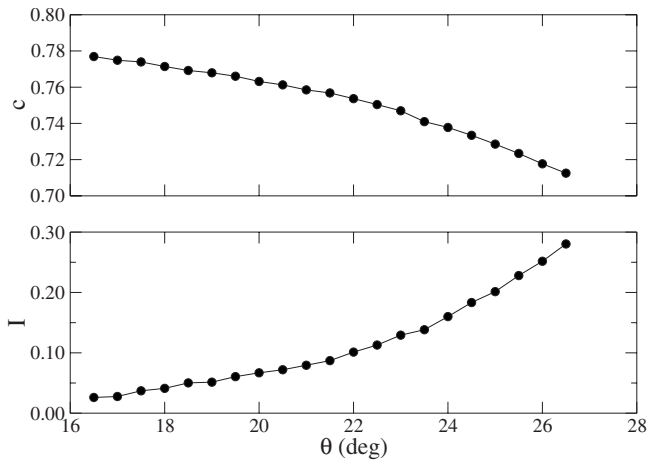

FIG. 4. Time-averaged inertia number I (bottom graph) and mean compacity c (top graph) as a function of the slope θ of the granular bed.

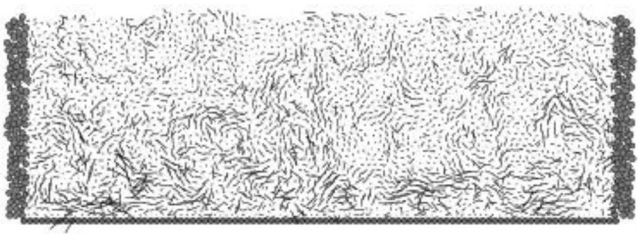

FIG. 5. Instantaneous grain velocity fluctuations in a stationary granular flow inclined at $\theta=20°$.

θ is displayed in Fig. 4, together with the variation of the time-averaged compacity c. As expected, I increases with θ, showing the increasing role of inertial effects on the dynamics. Simultaneously, the compacity decreases: the packing become less dense when flowing faster.

V. CORRELATIONS OF VELOCITY FLUCTUATIONS

At each time step t, the state of the flow is characterized by the position (x^i,y^i) and the velocity (v_x^i,v_y^i) of each grain i (although computed and available, we do not study in the following the rotational velocities ω^i). The instantaneous fluctuations of the velocities in the flow direction are computed for each grain: $\delta v_x^i=v_x^i-\langle v_x\rangle_{y^i}$, where $\langle v_x\rangle_{y^i}$ is the mean velocity in the x direction of the grains at a depth y^i in the layer (thus we account for the nonuniform velocity profile). In the same way, $\delta v_y^i=v_y^i-\langle v_y\rangle_{y^i}$. A typical snapshot of the instantaneous velocity fluctuations is shown in Fig. 5.

The mean velocity fluctuations of the grains averaged over the duration of the simulation, $\delta v_x=\Sigma_t\Sigma_i|\delta v_x^i|$, is computed in the bulk of the flow (at $y=h/2$) at the free surface and at the bottom. Normalized by $(gd)^{1/2}$, δv_x is plotted against the normalized mean velocity $V/(gh)^{1/2}$ for each value of the slope θ in Fig. 6. We observe that the amplitude of the velocity fluctuations is dependent on the depth, with larger fluctuations close to the bottom. At each depth, the points can be fitted by a power law, with the exponent α dependent on y: $\alpha=0.4$ at the free surface while $\alpha=0.63$ at the bottom (for comparison [11] finds $\alpha=0.7$ at the surface of

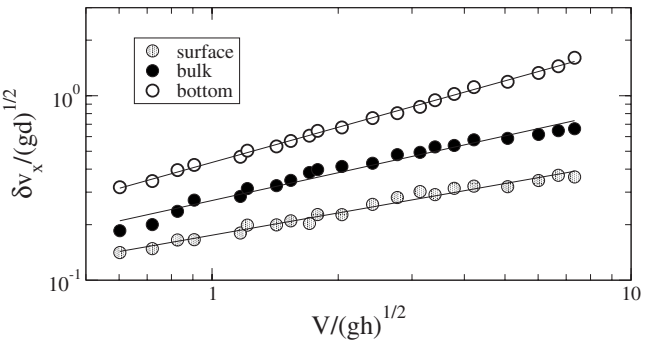

FIG. 6. Mean velocity fluctuations of the grains, $\delta v_x/(gd)^{1/2}$, as a function of the normalized mean flow velocity $V/(gh)^{1/2}$ in the bulk of the flow (dark circles), at the free surface (gray circles), and at the bottom (open circles). The straight lines show the power-law approximation, with exponents of, respectively, 0.50, 0.63, and 0.4.

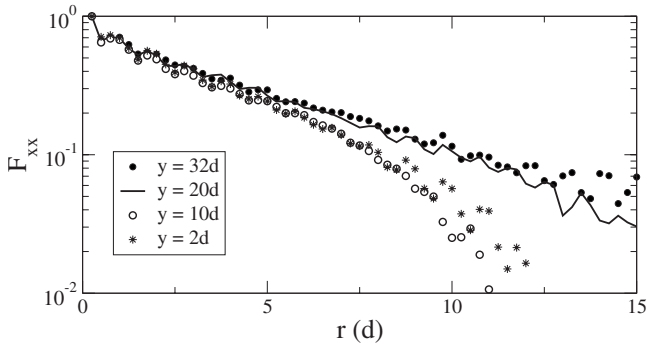

FIG. 7. Example of correlation functions $F_{xx}(r,y_0)$ computed for $y_0=32d$ (i.e., at the free surface), $y_0=20d$, $y_0=10d$, and $y_0=2d$ (i.e., at the bottom) for $\theta=17°$.

chute flows). The influence of the depth on the amplitude of the fluctuations will not be further discussed in the following; we limit our conclusion to the fact that velocity fluctuations are controlled by the shear rate in the bulk as well as at the free surface.

To establish the existence of a correlated motion of the grains in the bulk of the flow, we now compute the correlation functions relatively to the spatial distribution of the grain instantaneous velocity fluctuations. Two cases only are considered: namely, the correlation of the x and y velocities along the x direction. Indeed, the existence of a nonuniform velocity profile makes the computation of correlations in the y direction uncertain, at any rate noisy. For the same reason, correlation functions are computed at a given depth y_0 rather than averaged for the whole layer depth h. The correlation function reads

$$F_{xx}(r,y_0)=\frac{\sum_t\sum_{i,j}\delta v_x^i\delta v_x^i\Pi(x_{ij}-r)\Pi(y^i-y_0)\Pi(y^j-y_0)}{\sum_t\sum_{i,j}\Pi(x_{ij}-r)\Pi(y^i-y_0)\Pi(y^j-y_0)},$$

where $\Pi(x)$ is a step function taking the value 1, where $|x|<d/2$, and 0 otherwise. The function $F_{xy}(r,y_0)$ follows the same expression.

In a first step, in order to evaluate the influence of the choice of y_0 on F, we compute the function F_{xx} for y_0 varying between 0 and h, and for the two cases $\theta=17°$ and $\theta=23°$. Examples of the shape of the function F_{xx} are displayed in Fig. 7. For $r<8d$, they are well approximated by the exponential functions $F_{xx}(r)=A\exp(-r/\lambda_{xx})$, from which the correlation length λ_{xx} is directly inferred. We can thus plot λ_{xx} as a function of y_0 (Fig. 8). To allow for a reasonable evaluation of the dispersion of the values of λ_{xx}, the function F_{xx} is computed over successive time intervals of $14\sqrt{d/g}$ (corresponding data points represented in gray) and on a complete simulation duration of $70\sqrt{d/g}$ (corresponding data points shown in black). From Fig. 8, we observe (in spite of the important dispersion of the data) the weak yet existing influence of the depth y_0 on the correlation length λ_{xx}. Although insufficient to draw conclusions on this very aspect, our simulations suggest that correlations are of a smaller range in depth, presumably due to the grain agitation induced by the roughness and rigidity of the bottom. A different conclusion is drawn by Baran *et al.* [13], who found smaller correlations ($<1d$) close to the free surface. Further work would be required to completely address this issue. However, we can conclude from Fig. 8, first, that correlations over several grain diameter exist and, then, that F_{xx} can be *a priori* computed anywhere in the bulk without specific precaution.

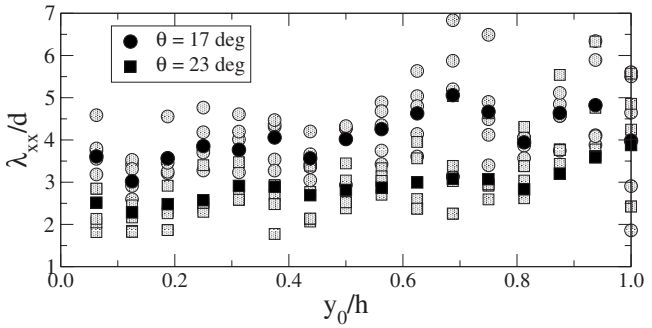

FIG. 8. Correlation length λ_{xx} as a function of the position y_0 in the flow for $\theta=17°$ and 23°; gray symbols stand for measurements over shorter time intervals (1 s), while black symbols coincide with the whole duration of the flow (namely, 5 s).

Focusing now on the influence of the slope on the spatial correlations of the velocity fluctuations, we arbitrarily set y_0 to the value of $20d$ (namely, $\simeq 2/3h$) and compute the function F_{xx} over the range of slope angle for which a stationary flow regime is reached. The resulting dependence $\lambda_{xx}(\theta)$ is displayed in Fig. 9. It clearly shows that for small slopes, correlations can exist over up to 6 grain diameters and that the correlation length decreases with increasing slope (although not below $2d$). The same conclusion holds for $y_0=10d$. The computation of correlation lengths λ_{xy} related to the velocity fluctuations in the y direction leads to the same observation, only on a smaller range (from $2d$ to $1d$). Figure 9 thus shows unambiguously the existence of correlated motion in the bulk of stationary dense granular flows, with a range of correlation varying on average between $4.5d$ and $2d$ inversely with the slope (namely, the shear rate). These results corroborate previous observation of correlated motion at the surface of dense granular flows [11].

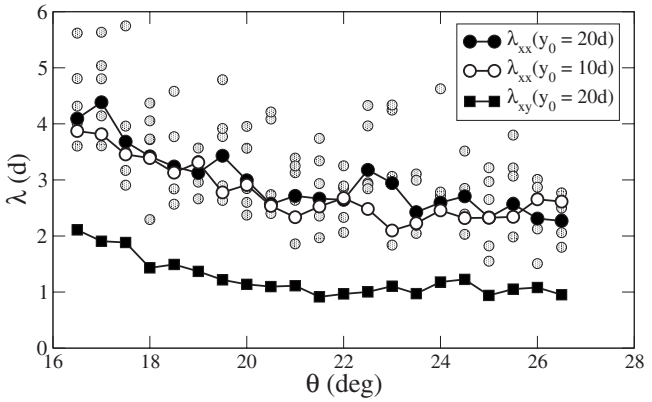

FIG. 9. Correlation length λ_{xx} as a function of the slope θ for $y_0=20d$ and $y_0=10d$ and λ_{xy} for $y_0=20d$; gray symbols stand for measurements over 1 s, while black symbols coincide with the whole duration of the flow, 5 s.

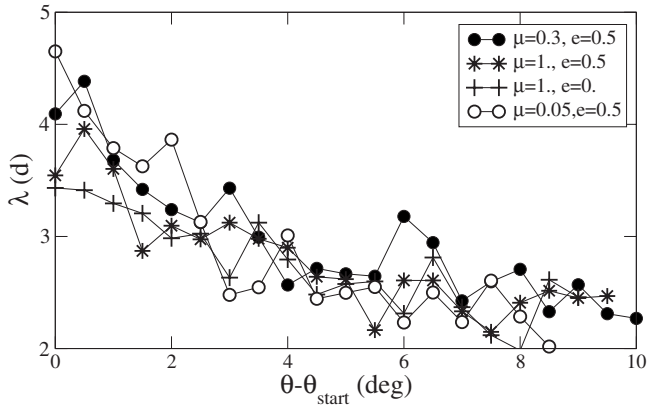

FIG. 10. Correlation length λ_{xx} as a function of the slope θ for $y_0=20d$ and different values of the contact coefficient of friction, μ, and coefficient of restitution, e.

VI. INFLUENCE OF GRAIN PROPERTIES

In order to investigate the role of material properties on the correlation of velocity fluctuations, series of simulations with different coefficient of friction μ and coefficient of restitution e between the grains were also carried out. While these parameters were set to $\mu=0.3$ and $e=0.5$ in the simulations discussed above, we now consider runs with $\mu=1$ and $e=0.5$, with $\mu=1$, $e=0$ and $\mu=0.05$, $e=0.5$. As previously, the correlation function F_{xx} is computed over the whole duration of the simulations and at a depth $y=20d$. The corresponding correlation length $\lambda_{xx}(y_0=20d,\mu,e)$ is plotted against $(\theta-\theta_{start})$ in Fig. 10; surprisingly, the material parameters μ and e seem to have only a negligible influence on the range of correlations. While the influence of the coefficient of restitution between the grains e on the macroscopic behavior of a granular mass is known to be negligible as long as e does not tends toward 1, this is not the case for the microscopic coefficient of friction μ. The fact that μ, though varying in a wide range, does not significantly affect the value of the correlation length associated with the grain velocity fluctuations is thus a bit surprising. At any rate it implies that λ is not reflecting the properties of the flowing granular matter.

VII. DISCUSSION

In this contribution, we have shown the existence of correlated motion of grains over several grain diameters in the bulk of stationary flows, analyzing the correlations of the instantaneous velocity fluctuations. The associated correlation length λ is shown to decrease with increasing shear rate. It is tempting to relate the existence of this correlated motion with the phenomenology of the flows: as suggested in [11], the h_{stop} function could result from variations of the correlation length λ with the shear rate. For the series of simulations with $\mu=0.3$ and $e=0.5$, h_{stop} is approximated using Eq. (1) where θ_1 and θ_2 are taken equal to the boundaries of the range of slopes for which stationary flow regime is possible: namely, 16.2° and 26°. Plotting $h_{stop}(\theta)$ against $\lambda_{xx}(\theta)$ shows a positive correlation, however too vague to make conclusions (Fig. 11). A positive correlation, yet closer to an exponential dependence, was observed as well in [13]. Moreover, investigating the role of grain properties μ and e, we show that the correlation length does not depend on the material properties.

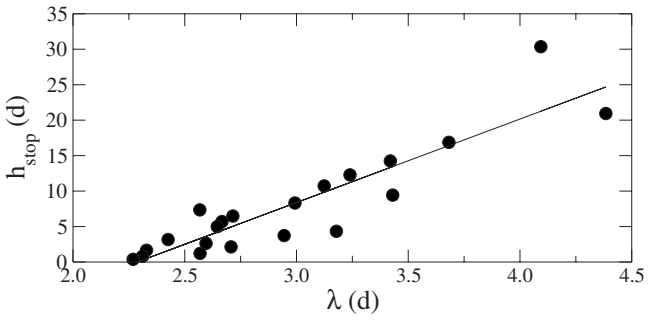

FIG. 11. Deposit function $h_{stop}(\theta)$ as a function of the correlation length $\lambda_{xx}(\theta)$

Relating the existence of correlated motion of grains and the associated typical length λ to the properties of the flow is thus far from straightforward. One could expect the local density to influence the value of λ: a close packing would indeed favor long-range interactions between the grains more efficiently than a looser packing would. However, plotting λ as a function of the compacity c for different slopes θ and for different material parameters μ and e shows that c does not alone control the value of λ (Fig. 12). On the other hand, plotting λ as a function of the inertia number I is more convincing (Fig. 13): we observe at first order a similar dependence for the different series of simulations. This reflects the fact that the correlation length decreases with the shear rate. However, further work should be carried out to address completely this issue.

While evidence of the existence of correlated motion of grains in the bulk of dense granular flows is given, many questions remain. First, the influence of the depth should be investigated; though our results reveal only a weak effect, we can nevertheless expect to meet its signature in the spatial organization of the correlated motion, granular flow properties being dependent on the nature of the underlying rough incline [18]. Another important aspect are the material properties μ and e; since they play a role in the flow rheology, the

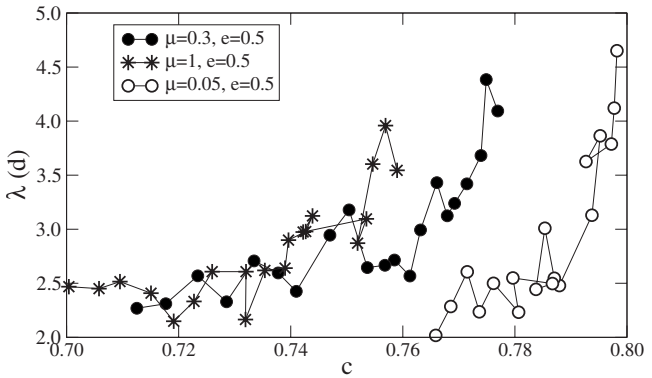

FIG. 12. Correlation length λ_{xx} as a function of the mean packing compacity for different values of the contact coefficient of friction, μ.

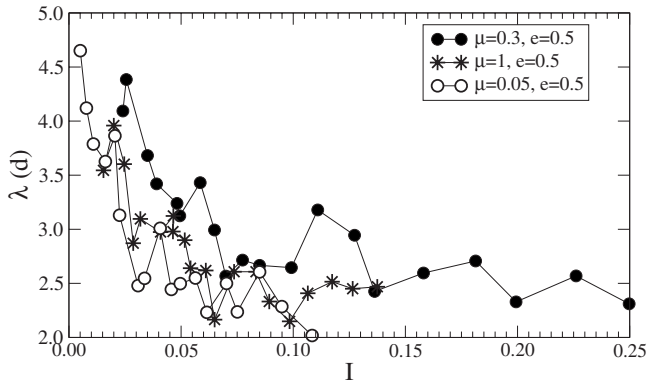

FIG. 13. Correlation length λ_{xx} as a function of the inertial number I for different values of the contact coefficient of friction, μ.

fact that they affect the correlation length only in a marginal way is puzzling. Their seemingly weak influence on the spatial correlations of the instantaneous velocity fluctuations suggests that time correlations should be considered. Whether the life span of clusters of correlated grains depends on their size and depth or on the grain properties is an open question which might help selecting length scales using more relevant criteria than spatial correlations only. At any rate, exploring this aspect would open important new prospects toward a better understanding and modeling of dense granular flows.

ACKNOWLEDGMENTS

The author thanks D. Lhuillier and P-Y. Lagrée for useful suggestions and comments on this work.

[1] GdR Midi, Eur. Phys. J. E **14**, 341 (2004).
[2] C. Josserand, P.-Y. Lagrée, and D. Lhuillier, Eur. Phys. J. E **14**, 127 (2004).
[3] I. S. Aranson and L. S. Tsimring, Phys. Rev. E **65**, 061303 (2002).
[4] T. Borzsonyi and R. E. Ecke, Phys. Rev. E **76**, 031301 (2007).
[5] L. E. Silbert, D. Ertas, G. S. Grest, T. C. Halsey, D. Levine, and S. J. Plimpton, Phys. Rev. E **64**, 051302 (2001).
[6] P. Jop, Y. Forterre, and O. Pouliquen, Nature (London) **441**, 727 (2006).
[7] J. Rajchenbach, Phys. Rev. Lett. **88**, 014301 (2001).
[8] B. Andreotti, A. Daerr, and S. Douady, Phys. Fluids **14**, 415 (2002).
[9] O. Pouliquen, Phys. Fluids **11**, 542 (1999).
[10] D. Ertaş and T. C. Halsey, Europhys. Lett. **60**, 931 (2002).
[11] O. Pouliquen, Phys. Rev. Lett. **93**, 248001 (2004).
[12] A. V. Orpe and A. Kudrolli, Phys. Rev. Lett. **98**, 238001 (2007).
[13] O. Baran, D. Ertaş, T. C. Halsey, G. S. Grest, and J. B. Lechman, Phys. Rev. E **74**, 051302 (2006).
[14] D. Bonamy, F. Daviaud, L. Laurent, M. Bonetti, and J. P. Bouchaud, Phys. Rev. Lett. **89**, 034301 (2002).
[15] J.-J. Moreau, Eur. J. Mech. A/Solids **4**, 93 (1994).
[16] L. Staron and E. J. Hinch, J. Fluid Mech. **545**, 1 (2005).
[17] M. Jean and J.-J. Moreau (unpublished).
[18] C. Goujon, N. Thomas, and B. Dalloz-Dubrujeaud, Eur. Phys. J. E **11**, 147 (2003).